

1 **Surface adhesion measurements in aquatic biofilms using**
2 **magnetic particle induction: MagPI**

3
4 Fredrik Larson^{1,2}, Helen Lubarsky¹, David M Paterson ^{*1}, Sabine U Gerbersdorf^{1,3}

5
6 ¹⁾ Sediment Ecology Research Group, Gatty Marine Laboratory, University of St
7 Andrews, East Sands, St Andrews, Fife KY16 8LB, Scotland, UK

8 ²⁾ Present address: Swedish Board of Fisheries, Research Office, Box 423, 401 26 L,
9 Sweden

10 ³⁾ Present address: Institute of Hydraulic Engineering, Universität Stuttgart,
11 Pfaffenwaldring 61, 70569 Stuttgart, Germany

12
13
14
15
16
17
18 *Corresponding author, E-mail: dp1@st-andrews.ac.uk

19
20 Running head: Magnetic Particle Induction

21 Acknowledgements

22 The concept of using test particles and electromagnets for measurements of biofilm
23 adhesion was developed by Professor David M. Paterson while working under the auspices of
24 the RIBS (Research Initiative on Bahamian Stromatolites) programme funded by the NSF,
25 USA. This is publication No XXX of the RIBS programme. Test particles were supplied
26 through Partrac, UK (http://www.partrac.com/content/01_home.php) and their help in
27 developing the materials is gratefully acknowledged. Funding for the post-doctoral
28 scholarship to F. Larson was received from the Swedish Research Council for Environment,
29 Agricultural Sciences and Spatial Planning (Formas). H. Lubarsky was funded by a EU
30 research training network (MRTN-CT-2006-035695), S U. Gerbersdorf was funded by a
31 Marie Curie Intra-European Fellowship (European Commission, FP6, Project BioMech). We
32 would like to thank G. Lubarsky and L. Kirk at the department of Physics and Astronomy at
33 the University of St Andrews and M. Chocholek of Geosciences for valuable input and
34 assistance with the magnet tests and calibrations and also Dr Alan Decho (University of
35 South Carolina) for his kind permission to use the confocal images.

36 Abstract

37 Sediment stability is a product of interacting physical and biological factors and while
38 stability can be measured, few techniques allow sensitive assessment of the sediment surface
39 as conditions change. For example, stability gradually increases as a biofilm develops, as
40 salinity rises, or may be influenced by toxic compounds. This paper introduces a new
41 technique (Magnetic Particle Induction: MagPI) based on the magnetic attraction of specially-
42 produced fluorescent ferrous particles. The test particles are added to a surface and subjected
43 to an increasing magnetic field, using either a permanent magnetic or a variable
44 electromagnet. There is a strong correlation between magnetic flux density and distance from
45 the surface ($r^2 = 0.99$) for the permanent magnets and for the magnetic flux density and the
46 current supplied to electromagnets ($r^2 > 0.95$). The magnetic force at which the particles are
47 recaptured from the surface is determined as a measure of the adhesive nature of the surface.
48 MagPI therefore determines the “stickiness” of the surface, whether a biofilm, a sediment or
49 other material. The magnetic flux density (mTesla) required to remove test particles from
50 diatom biofilms (mean 15.5 mTesla) was significantly greater than from cyanobacterial
51 biofilms (mean 10 mTesla). Controls of fine glass beads showed little adhesion (mean 2.2
52 mTesla). Surface adhesion is an important bed property reflecting the sediment system’s
53 potential to capture and retain new particles and accumulate material. The methodology is
54 dynamic, provides high precision, and is easily controlled. MagPI offers a straight forward
55 and economic way to determine the surface adhesion of a variety of surfaces rapidly and with
56 precision. The technique may have applications in physical, environmental and biomedical
57 research.

58 Introduction

59 Biofilms are close to omnipresent in benthic aquatic systems and important in many
60 scientific disciplines including medical research (Guo et al. 2008; Jain et al. 2007; Morton et
61 al. 1998), waste-water treatment (Liu and Fang 2003; Raszka et al. 2006), toxicant removal
62 (Sheng et al. 2008) and biotechnology (Flemming and Wingender 2001; Sutherland et al.
63 1998). Considerable interest has focused on the importance of biofilms for increasing
64 sediment stability through the mechanical effects of the microbially-produced matrix of
65 extracellular polymeric substances (EPS, reviewed in Stal 2003; Underwood and Paterson
66 2003). Sediment stability is a governing factor in sediment management because sediment
67 transport and the release of associated contaminants have important consequences for the
68 ecological and commercial health of aquatic habitats from the watershed to the sea (Förstner
69 et al. 2004; Paterson et al. 2000). To assess the potential sediment erosion risk under
70 hydrodynamic forcing, several devices have been developed to determine “the critical erosion
71 threshold” (τ_{crit}) for sediment transport and the erosion rates (ϵ) of natural sediments. The
72 critical erosion threshold is often an operational threshold defined by the characteristics of the
73 chosen device rather than the actual theoretical point of incipient sediment motion (Tolhurst
74 et al. 2000) This is partly because erosion devices are based on many different approaches
75 including water flow (e.g. Sedflume, McNeil et al. 1996); SETEG, Kern et al. 1999), water
76 jets (CSM, Paterson 1989), oscillation of a horizontal grid (Tsai and Lick 1986), a propeller
77 (EROMES, Schuenemann and Kuehl 1991), or combined suction and flow (Gust-Microcosm,
78 Gust and Mueller 1997).

79 While these methods all provide important information on the erosional behaviour of the
80 sediment, they all require that bed failure occurs and therefore cannot measure any changes in
81 surface properties below the point of incipient erosion. This restricts their use and because
82 depositional beds must usually resist erosion to exist, this leaves a large gap in our knowledge

83 and consequently more sensitive methods are needed. MagPI measures a different property of
84 the sediment surface and thus does not replace erosion devices, but provides a framework for
85 a sensitive analysis of surface adhesive capacity, a useful addition to the properties of the bed
86 that can be determined.

87 The use of magnetism in various forms of bacterial biofilm research is widespread.
88 Magnetic resonance imaging (MRI) has been used to visualise structure and detachment of
89 biofilms (Manz et al. 2005; McLean et al. 2008), while surface bio-magnetism has been used
90 to change cell adhesion and protein secretion (Chua and Yeo 2005). Immobilisation of
91 magnetic particles by aggregates of pathogenic bacteria has been employed to assess biofilm
92 formation in microtitre plates (Chavant et al. 2007). The new MagPI approach is based on the
93 finding that the force needed to retrieve magnetic particles from a biofilm is a sensitive
94 indicator of retentive ability or adhesive capacity of the substratum and a proxy for sediment
95 “stability”. MagPI may also prove to be a possible index for other well-known features of a
96 biofilm such as the potential to capture particulate-associated pollutants, binding of nutrients
97 or the incorporation of deposited sediment particles, although this will require more research.

98 For the methodology demonstrated presented here, two types of magnets were used:
99 permanent magnets and electromagnets. In both cases, a defined volume of magnetic particles
100 (of known size range and density) were spread in a single layer onto a defined area of the
101 submerged sediment surface and the force of the overlying magnet was increased until the
102 particles were recaptured. The magnetic force was gradually enhanced by either reducing the
103 distance between the magnet and the test particles (permanent magnet), or by increasing the
104 electrical current to a variable magnet statically positioned 5-10 mm above the sediment
105 (electromagnet). The sensitivity of this method has been illustrated by data presented for
106 developing microalgal (diatoms and cyanobacteria) biofilms. The magnetic devices were
107 found to be economically viable, easy to build and the Gauss Meter enables comparison of

108 results gained in different devices/experiments/laboratories. The relative merits and the use of
109 the two types of magnets (field, laboratory) are discussed.

110 Materials and Procedures

111 *Magnetic particle induction*

112 *Permanent neodymium magnets*— After extensive testing of a variety of permanent
113 magnets, Neodymium alloy (NdFe₃B) disc-magnets were chosen for their superior magnetic
114 strength, Nd being the most magnetic element found on earth (Coey 1995; Lebech et al.
115 1975). The Nd disc-magnets (20 × 5mm: e-magnets, UK) were applied either individually or
116 as a stack of up to five, depending on strength requirements. Adding any more than 5 disc
117 magnets did not increase the active magnetic field interacting with the test surface. The force
118 from the permanent magnets acting upon the surface was regulated using decreasing distance
119 to the bed controlled by an adjustable vernier-scaled manipulator (Fig. 1).

120

121 *Electromagnets*— The electromagnets were controlled by a precision power supply to
122 allow fine and precise variation of voltage and current (Rapid 5000 variable power supply)
123 (Fig. 1). A wide range of commercially available electromagnets was tested, but none showed
124 the required functionality. The most common problems of commercial magnets were either in
125 their size, obscuring the test surface or insufficient strength to retract the test particles from
126 different surfaces. Thus, purpose-made electromagnets were constructed by using metal cores
127 of ferrous alloy coiled with insulated copper thread. To increase the overall range of the
128 magnetic field, two magnets were constructed covering a complementary range of magnetic
129 forces. The magnets had metal cores of 10 mm and 5 mm diameters and were each coiled
130 with 500 turns of copper thread with a diameter of 0.4 mm and 0.2 mm, respectively. The coil
131 covered 60mm of the core on both magnets. The full coil resistance of the larger
132 electromagnet was 35 Ω, and it was limited to an input range of 0-12 V (0-0.34 A). The

133 smaller magnet had a coil resistance of 24 Ω and was limited to an input range of 0-20 V (0-
134 0.83 A). Exceeding these limits burnt the coils, since above this level of supply increased
135 current was dissipated as heat due to electrical resistance.

136 *Ferrous test particles*— The test particles consisted of an amalgam of ferrous material to
137 provide a magnetic response, mixed with fluorescent pigment to increase their visibility (Fig.
138 2). An inert transparent binding agent combines the material into a solid which is then ground
139 to produce a particle spectrum (Partrac, UK). The test particles were then sieved into different
140 size classes. The size range selected for the trials was 180-250 μm , similar to fine/medium
141 beach sand. The particles have to be applied to the test surface in consistent manner to allow
142 repeatable measurements. To achieve a relatively even single layer of particles on the test
143 surface took some practise but was achieved with experience. The test particles were
144 suspended in water and the mixture drawn into a plastic pipette. The suspended particles were
145 allowed to settle towards the tip of the pipette before being ejected as a single drop in the
146 media above the test surface. A cut-off 2ml syringe, submerged into the water and held a short
147 distance above the test surface, served as a guide to confine the particles to the selected test
148 area.

149 *Calibrations*— To calibrate the device, the magnets were placed over a Hall sensor
150 connected to a Gauss Meter (Unilab, Blackburn, England). The permanent magnets were
151 lowered towards the probe in incremental steps (1 mm). The magnetic flux density (MFD) in
152 mTesla was recorded for each step. For the electromagnets, the voltage and current was
153 increased in small increments (0.2 V / \approx 0.05 A) and the MFD for each increase was recorded.
154 The Hall sensor calibrations were performed in air as well as submerged in water using a
155 waterproof sensor. Calibrations were performed both before and after each experiment.
156 During the experiment, the resistance of electromagnets was regularly checked. A decrease in
157 coil resistance would be evidence of a fault which results in a loss of magnetic field strength.

182
$$F = \frac{\mu^2 N^2 I^2 A}{2\mu_0 L^2} \quad \text{Equation 2}$$

183 where μ is the permeability of the core material, N is the number of thread turns in the coil, I
184 is the current, A and μ_0 as above, and L is the full length of the thread used in the coil
185 (Breithaupt 1999b). Consequently, the magnetic force (F) can be controlled by varying the
186 current (I) while all other factors are held constant.

187

188 *Precision and Statistics*— The precision of the method was tested through repeated
189 calibrations (n=25). Based on 95 % confidence intervals, an average precision of 0.1% for the
190 electromagnet measurements was determined (± 0.22 % in the low current range, ± 0.035 %, in
191 the mid current range and ± 0.045 % in the high current range). The use of a different
192 electromagnet and/or other power source requires a separate precision test to be conducted,
193 but as long as a suitably sensitive power supply is used, a similar range could be expected.
194 Data was assessed for normality and homogeneity of variance and then a one-way ANOVA
195 was applied (significance level of $\alpha = 0.05$) and post-hoc test (Tukey) to determine
196 differences in surface adhesion between varying surfaces and biofilm compositions.

197 *Calibration results*— There were strong linear relationships ($r^2 = 0.996-0.997$) between
198 current (I) and the magnetic flux density (mTesla) for the electromagnets. The relationship
199 between distance and magnetic field strength of the permanent magnets was exponential (Fig.
200 3). In contrast to the electromagnets, the permanent magnets have to be moved towards the
201 surface during the measurement to increase F. Consequently, the area of the magnetic field
202 that interacts with the surface increases with decreasing distance and this corresponds to a
203 non-linear increase of the field strength (Fig. 3a). The line of best fit for the calibration of the
204 permanent magnet strength versus distance required a sixth order polynomial as opposed to
205 the linear function used for the electromagnet calibration (Fig. 3a).

206 *Abiotic particulate surfaces*—Substrata of different types and particles sizes were tested
207 during the pilot studies: two size fractions of clean glass beads (<63 μm and >150 μm
208 Ballotini™ beads), as well as sand and mud which had been furnaceed to remove organic
209 material. These substrata were submerged in both seawater and freshwater to take into
210 account any ionic interactions.

211 *Biofilm surface testing*— The influence of biotic surfaces was examined using cultured
212 biofilms of benthic cyanobacteria (dominated by *Oscillatoria* spp.) and pennate diatoms
213 (dominated by *Nitzschia* spp.). Both cultures were grown on clean glass beads (<63 μm
214 Ballotini™) in a temperature-controlled room (15°C) under a 13 h/11 h light/dark cycles
215 (~250 $\mu\text{mol m}^{-2} \text{s}^{-1}$). Similar glass beads covered with pre-filtered (1 μm), autoclaved
216 seawater without microalgal inoculums served as a control. For the treatments and the
217 controls, plastic weighing trays (55 × 55 × 23 mm) were filled with a 5mm layer of the <63
218 μm glass beads and filled with autoclaved seawater. The experimental period covered 19 days
219 to follow changes in the surface properties of developing biofilm cultures. The small
220 electromagnet described above was employed for these tests.

221 *Threshold conditions*— In terms of the thresholds of test particles response to magnetic
222 force, the total clearance (D) was the preferred measure. Firstly, this threshold is the least
223 subjective and the data gained by different persons are almost identical and secondly, this
224 threshold showed significant differences between treatments, which were not always obvious
225 using the other three thresholds (Fig. 4). Under laboratory condition, where more
226 sophisticated observation using microscopy of the particles is possible, the first and second
227 threshold can be used as an alternative and/or complementary value. In general terms, we
228 recommend recording all thresholds if possible as each may indicate a slightly different
229 property of the surface.

230

231 Assessment

232 *Abiotic particulate surfaces*— The force required to recapture the test particles (size 180-
233 250 μm) from various substrata are given (Fig. 5). Measurements indicated differences
234 between seawater and freshwater conditions. Under seawater, it was more difficult to capture
235 test particles from the bed composed of larger glass bead than from the smaller glass beads,
236 followed by mud and then the cleaned sand (Fig. 5a). Under freshwater conditions, the
237 magnetic force needed to retrieve the test particles was similar for all surfaces except the
238 larger glass beads which showed a significantly higher “retentive capacity” (Fig. 5b).

239

240 For the sand, similar forces were needed to retrieve particles in seawater and freshwater,
241 but relatively greater force had to be applied in seawater to recapture particles from the other
242 substrata (compare Fig. 5a and b). This is probably due to the ionic nature of seawater
243 increasing the potential for electrostatic and other physico-chemical attractions between
244 particles (e.g. mud with silt and clay content known for their surface charge variation). This
245 could imply that the ionic milieu facilitates the cohesion of the surface as measured by
246 MagPI. However, increased binding capacity was also noted in freshwater from the larger
247 glass bead substratum. This may be because the magnetic particles become physically
248 trapped in the pore spaces between the larger glass beads. However, both the smaller and
249 larger glass beads showed enhanced surface cohesion in seawater as opposed to freshwater
250 which suggests both mechanisms may be responsible for the binding capacity of the larger
251 glass beads.

252 *Biotic experiment example*— The biotic test experiments revealed that the biofilms
253 developed by benthic diatoms under these conditions had a more adhesive surface compared
254 to the cyanobacterial biofilms (Fig. 6). One plausible explanation for this was that the
255 experimental irradiance was relatively high and cyanobacteria, in this case dominated by

256 *Oscillatoria* spp., tend to prefer lower light levels, thus forcing them deeper into the sediment
257 matrix and reducing surface EPS production. Diatoms, in contrast, are better adapted to higher
258 irradiances. The important aspect was that the MagPI method was able to detect even quite
259 small differences in surface adhesion with high precision (Fig. 6).

260

261 Discussion

262 *Application and replication of the method*— The equipment required for the method
263 described here is simple and affordable (Figs. 1 and 2). However, production of suitable
264 electromagnets does demand some technical understanding to achieve the acquired magnetic
265 strength.

266 In the laboratory, electromagnets were preferred over permanent magnets due to the
267 accuracy of their calibration and ease of deployment. Depending on the design and power
268 source, electromagnets offer the possibility to increase the magnetic force in small steps, thus
269 offering a high resolution within the applied magnetic strength range. A fixed distance marker
270 (non-metallic) fitted at the tip of the electromagnet helps to ensure positional accuracy
271 between measurements. Permanent magnets are recommended for measurements in the field
272 (e.g. tidal flats) because of the logistical ease for field use. The permanent magnets still
273 produce an accurate and stable force at each set distance, although the precise manipulation of
274 the distance between the magnet and the test surface is critical. To ensure correct initial
275 placement, a small guide rod (glass or plastic, not metal) was used to set the magnet the
276 desired initial distance from the surface (cf 2 cm). The vernier scale ($\pm 100 \mu\text{m}$) was then
277 used to move the magnet in small incremental steps and the results recorded. The test surface
278 must be reasonably flat and the magnet face set parallel to the surface.

279 *Ferrous test particles* — The choice of the size of the test particles is an important
280 decision. It is sensible to select a size range of particles that does not deviate too much from

281 the test sediment, preferably being slightly larger to prevent trapping in surface pore space.
282 Although this type of trapping may not be an issue on surfaces where biofilm has developed,
283 the test particle size is also important for the ease of observation on the surface. It is also
284 sensible to use a narrow size range of test particles, to enhance the uniformity of the particle
285 interactions with the surfaces.

286 Another variable is the “incubation” time or period that particles are left on the test
287 surface before performing the measurement. Since this depends on the characteristics of the
288 investigated surface as well as on the objectives of a particular study, it should be decided by
289 the operator on the basis of the question to be addressed in each experiment. The simplest
290 way to ensure a repeatable measure of the test surface is to retract particles directly after their
291 addition and the most appropriate value of the surfaces “stickiness” can be gained directly
292 after adding the particles. When particles are left for a longer time, they will be partly or fully
293 incorporated in the biofilm and the measured variable becomes a combination of the adhesion
294 of the surface and the capacity to entrap particles by biofilm development (Fig. 2 E).
295 However, we can envisage experiments (and have begun to conduct them) where particles are
296 added and time after addition is an important variable of interest.

297

298 Comments and recommendations

299 *Advantages and limitations*— A great advantage of MagPI is the ability to measure
300 biofilm adhesion, a variable that has rarely been considered, but is at the same time of great
301 significance for binding pollutants, trapping nutrients, enhancing sediment stability and
302 capturing new deposited particles. For instance, the “ecosystem service” (Paterson et al. 2008)
303 of particle capture and retention is of great importance to sediment systems in balancing the
304 replacement of material lost by tidal erosion (Verney et al. 2006) or wave action (Andersen et
305 al. 2007), enhancing the nutrient status (Freeman and Lock 1995) and offering binding sites

306 for pollutants (Ghosh et al. 2003). This biofilm adhesion can be measured with high
307 sensitivity and small changes in developing biofilms can be demonstrated which would be
308 unnoticed using established erosion devices. MagPI comes at comparatively low cost, and
309 with basic practical skills and technical understanding it is comparatively easy to build and
310 use.

311 Although the permanent magnet is valuable for the use in the field, MagPI cannot easily
312 be used if a wet biofilm is not submerged, such as during tidal emersion periods. The
313 measurements have to be performed underwater by the help of a water-filled chamber,
314 otherwise the magnetic particles interact with the surface tension of the water-film and these
315 forces confound the measurement of adhesion.

316

317 *Other possible applications*— This method can be used for any sub-tidal or intertidal
318 sediments, including complex biofilm-based systems such as stromatolites (Paterson et al.
319 2008) but the measurements of moist surfaces should be made underwater because of surface
320 tension effects. In addition, dry exposed surfaces where adhesion is important might also be
321 examined, to-date we have tested very few other substrata, but stonework, tree surfaces,
322 leaves etc remain possible candidates for investigation.

323 The MagPI represents an economically viable, easily constructed, easy-to-use tool to
324 determine surface adhesion, a proxy for the retentive capacity of the substratum. The
325 knowledge of surface adhesion can provide useful insights for particulate pollutant capture,
326 nutrient trapping, enhancing sediment stability and capturing particles in various depositional
327 systems such as intertidal flats, shallow submerged sediment systems and stromatolites to
328 name but a few. In contrast to established erosion devices, MagPI can determine small
329 changes in surface properties below the point of incipient erosion with high sensitivity, high
330 accuracy and a high repeatability. The calibration by the Gauss meter makes the comparison

331 of the data between different experiments and various laboratories possible, which is an
332 important prerequisite for future success in biofilm research. Two types of magnets have been
333 examined here: the high power permanent magnet for increased mobility and application in
334 the field and the electromagnet which is to be preferred in the laboratory due to a higher
335 accuracy in calibration and measurement. The technique presented here is likely to have
336 future applications in environmental, medical and biotechnological research.

337

338 References

- 339 Andersen, T. J., J. Fredsoe, and M. Pejrup. 2007. In situ estimation of erosion and deposition
340 thresholds by Acoustic Doppler Velocimeter (ADV). *Estuarine Coastal and Shelf*
341 *Science* 75: 327-336.
- 342 Breithaupt, J. 1999. *Magnetic Fields*, p. 251-263. Physics. MacMillan Publishers Ltd.
- 343 Chavant, P., B. Gaillard-martinie, R. Talon, M. Hebraud, and T. Bernardi. 2007. A new
344 device for rapid evaluation of biofilm formation potential by bacteria. *Journal Of*
345 *Microbiological Methods* 68: 605-612.
- 346 Chua, L. Y., and S. H. Yeo. 2005. Surface bio-magnetism on bacterial cells adhesion and
347 surface proteins secretion. *Colloids and Surfaces B-Biointerfaces* 40: 45-49.
- 348 Coey, J. M. D. 1995. Rare-earth magnets. *Endeavour* 19: 146-151.
- 349 Flemming, H. C., and J. Wingender. 2001. Relevance of microbial extracellular polymeric
350 substances (EPSs) - Part II: Technical aspects. *Water Science and Technology* 43: 9-
351 16.
- 352 Freeman, C., and M. A. Lock. 1995. The biofilm polysaccharide matrix - a buffer against
353 changing organic substrate supply. *Limnology and Oceanography* 40: 273-278.
- 354 Förstner, U., S. Heise, R. Schwartz, B. Westrich, and W. Ahlf. 2004. Historical contaminated
355 sediments and soils at river basin scale. *Journal of Soils and Sediments* 4: 247-260.
- 356 Ghosh, U., J. R. Zimmerman, and R. G. Luthy. 2003. PCB and PAH speciation among
357 particle types in contaminated harbor sediments and effects on PAH bioavailability.
358 *Environmental Science & Technology* 37: 2209-2217.
- 359 Guo, L. H., H. L. Wang, X. D. Liu, and J. Duan. 2008. Identification of protein differences
360 between two clinical isolates of *Streptococcus mutans* by proteomic analysis. *Oral*
361 *Microbiology and Immunology* 23: 105-111.

362 Gust, G., and Mueller. 1997. Interfacial hydrodynamics and entrainment functions of
363 currently used erosion devices. In: Burt, N., Parker, R., Watts, J. (Eds.), *Cohesive*
364 *Sediments*. Wiley, Chichester, pp. 149–175.

365 Jain, A., Y. Gupta, R. Agrawal, P. Khare, and S. K. Jain. 2007. Biofilms - A microbial life
366 perspective: A critical review. *Critical Reviews in Therapeutic Drug Carrier Systems*
367 24: 393-443.

368 Kern, U., V. Shuerlein, M. Holzwarth, I. Haag, and B. Westrich. 1999. Ein strömungskanal
369 zur ermittlung der tiefenabhängigen erosionsstabilität von gewassersedimenten: das
370 SETEG system. *Wasserwirtschaft* 89: 72-77.

371 Lebech, B., K. A. McEwen, and P. A. Lindgard. 1975. Magnetism in prasedymium-
372 nedymium single-crystal alloys. *Journal of Physics C-Solid State Physics* 8: 1684-
373 1696.

374 Liu, H., and H. H. P. Fang. 2003. Hydrogen production from wastewater by acidogenic
375 granular sludge. *Water Science and Technology* 47: 153-158.

376 Manz, B., F. Volke, D. Goll, and H. Horn. 2005. Investigation of biofilm structure, flow
377 patterns and detachment with magnetic resonance imaging. *Water Science and*
378 *Technology* 52: 1-6.

379 McLean, J. S., O. N. Ona, and P. D. Majors. 2008. Correlated biofilm imaging, transport and
380 metabolism measurements via combined nuclear magnetic resonance and confocal
381 microscopy. *Isme Journal* 2: 121-131.

382 McNeil, J., C. Taylor, and W. Lick. 1996. Measurements of erosion of undisturbed bottom
383 sediments with depth. *Journal of Hydraulic Engineering-Asce* 122: 316-324.

384 Morton, L. H. G., D. L. A. Greenway, C. C. Gaylarde, and S. B. Surman. 1998. Consideration
385 of some implications of the resistance of biofilms to biocides. *International*
386 *Biodeterioration & Biodegradation* 41: 247-259.

387 Paterson, D. M. 1989. Short-term changes in the erodibility of intertidal cohesive sediments
388 related to the migratory behavior of epipellic diatoms. *Limnology And Oceanography*
389 34: 223-234.

390 Paterson, D. M., Aspden, R.J., Visscher, P.T., Consalvey, M., Andres, M.S., Decho, A.W.,
391 Stolz, J. and Reid, R.P. 2008. Light-dependant biostabilisation of sediments by
392 stromatolite assemblages. *PLoS ONE* 3: e3176.
393 [doi:3110.1371/journal.pone.0003176].

394 Paterson, D.M., Tolhurst, T.J., Kelly, J., Honeywill, C., de Deckere, E.M.G.T., Huet, V.,
395 Shayler, S.A., Black, K.S., De Brouwer, and Davidson, I. 2000. Variations in
396 sediment properties, Skeffling mudflat, Humber Estuary, UK. *Continental Shelf*
397 *Research* 20: 1373-1396.

398 Raszka, A., M. Chorvatova, and J. Wanner. 2006. The role and significance of extracellular
399 polymers in activated sludge. Part I: Literature review. *Acta Hydrochimica Et*
400 *Hydrobiologica* 34: 411-424.

401 Schuenemann, M., and H. Kuehl. 1991. Experimental investigations of the erosional
402 behaviour of naturally formed mud from from the Elbe estuary and adjacent Wadden
403 sea, Germany, p. 314-330. *In* A. J. Mehta [ed.], *Nearshore and Estuarine Cohesive*
404 *Sediment Transport Workshop*.

405 Sheng, G. P., M. L. Zhang, and H. Q. Yu. 2008. Characterization of adsorption properties of
406 extracellular polymeric substances (EPS) extracted from sludge. *Colloids and Surfaces*
407 *B-Biointerfaces* 62: 83-90.

408 Stal, L. J. 2003. Microphytobenthos, their extracellular polymeric substances, and the
409 morphogenesis of intertidal sediments. *Geomicrobiology Journal* 20: 463-478.

410 Sutherland, T. F., J. Grant, and C. L. Amos. 1998. The Effect of Carbohydrate Production by
411 the Diatom *Nitzschia curvilineata* on the Erodibility of Sediment. *Limnology and*
412 *Oceanography* 43: 65-72.

413 Tolhurst, T., K. Black, D. M. Paterson, H. Mitchener, G. Termaat, and S. Shayler. 2000. A
414 comparison and measurement standardisation of four in situ devices for determining
415 the erosion shear stress of intertidal sediments. *Continental Shelf Research* 20: 1397-
416 1418.

417 Tsai, C. H., and W. Lick. 1986. A portable device for measuring sediment resuspension.
418 *Journal of Great Lakes Research* 12: 314-321.

419 Underwood, G. J. C., and D. M. Paterson. 2003. The importance of extracellular carbohydrate
420 production by marine epipelagic diatoms, p. 183-240. *Advances In Botanical Research*,
421 Vol 40. *Advances In Botanical Research Incorporating Advances In Plant Pathology*.

422 Verney, R., J. C. Brun-Cottan, R. Lafite, J. Deloffre, and J. A. Taylor. 2006. Tidally-induced
423 shear stress variability above intertidal mudflats in the macrotidal Seine estuary.
424 *Estuaries and Coasts* 29: 653-664.

425

426

427 Figures and figure legends

428

429 Figure. 1. Schematic diagram of the two variants of MagPI. Electromagnetic version (left)
430 with a variable current supply and permanent disc-magnets (right) using decreasing distance
431 to surface. In each case, fluorescent ferrous particles are added to the sediment surface. The
432 current input or the distance from the surface is recorded in each case, respectively, as the
433 particles respond.

434

435 Figure. 2. A: Prototype of MagPI placed above the surface of a sample of intertidal microbial
436 sediment (stromatolite) during the NSF RIBS programme (see acknowledgements). Test
437 particles can be seen adhering to the magnet. B: Sample of stromatolite prepared for MagPI
438 measurement. C: Detail of surface showing fluorescent particles among stalked diatoms on
439 one region of stromatolite. D and E: Confocal microscopy of fluorescent beads on the
440 stromatolite surface becoming incorporated into the biofilm. The green colouration represents
441 organic material while the red fluorescence represents the test particles. Note the test particles
442 are approximately 125-150 μm across in this example. (Bar markers: A = 1 cm, B = 5 cm, C =
443 5 mm, D = 150 μm , E = 150 μm). Confocal images supplied by Dr A. Decho.

444

445 Figure. 3. Examples of calibration curves for the permanent (A) and electromagnetic (B)
446 devices, respectively. A: An exponential increase in force as the permanent magnet
447 approaches the surface. B: The strong linear relationship between magnetic force and supplied
448 current for the electromagnet as the current was gradually increased. Black line- the magnet
449 was stationed 5 mm from the surface. Grey line- the magnet was stationed 10 mm from the
450 surface.

451

452 Figure. 4. The thresholds used in the magnetic measurements (A) particle orientation to
453 magnetic field, (B) first magnetic particle captured by the magnet, (C) larger groups of
454 particles attracted and finally (D) total clearance of particles under the magnet. Three
455 treatments are given as examples: Small glass beads submerged in seawater (SW) and
456 freshwater (FW) and large glass beads in SW using test particles of size range 180-250 μm .
457 $n=6$, SE-bars.

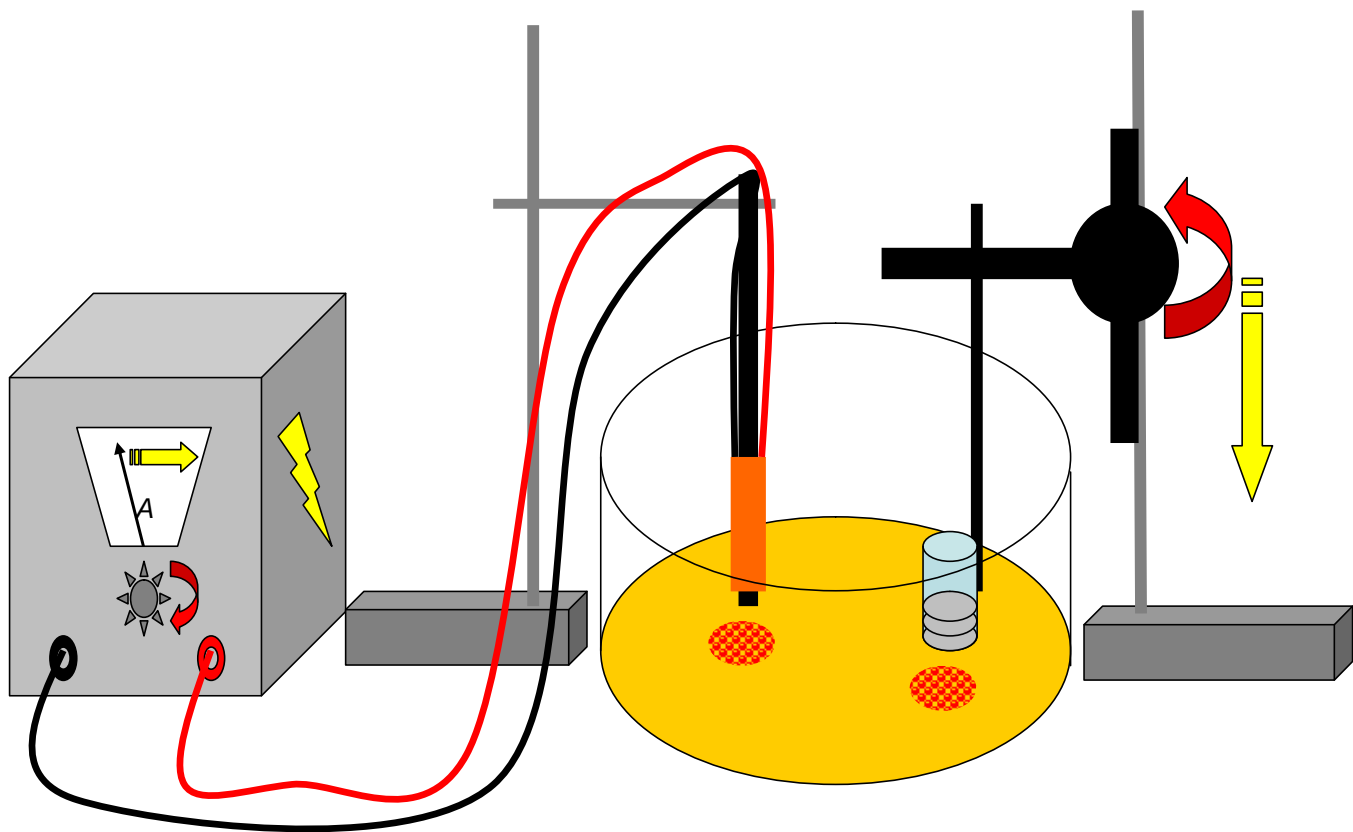
458

459 Figure. 5. Tests on abiotic particulate beds of different materials in (a) seawater and (b)
460 freshwater to attract test particles (180-250 μm) by MagPI ($n = 6$, $\pm\text{SE}$, * indicates significant
461 difference between adjacent groups by ANOVA, $\alpha = 0.05$ and subsequent Tukey test)

462

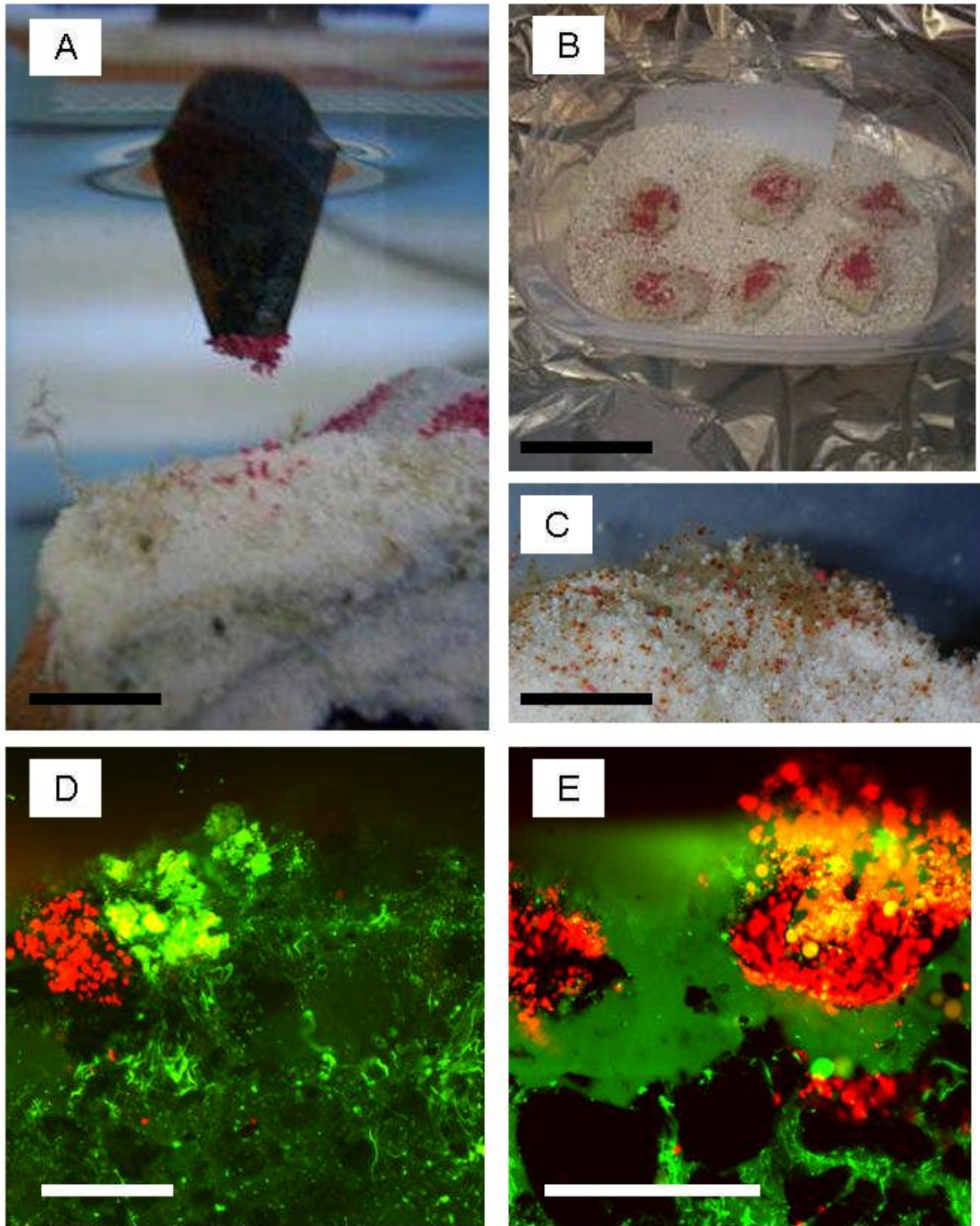
463 Figure. 6. Biotic example with cultured biofilms grown with diatoms and cyanobacteria,
464 respectively. The cyanobacterial biofilm had a lower surface adhesion than the diatom
465 biofilm. The threshold reported is the strength of the magnetic field needed to provide total
466 clearance of particles under the magnet ($n = 6$, $\pm\text{SE}$, * indicates significant difference
467 between groups by ANOVA, $\alpha = 0.05$ and subsequent Tukey test)

468



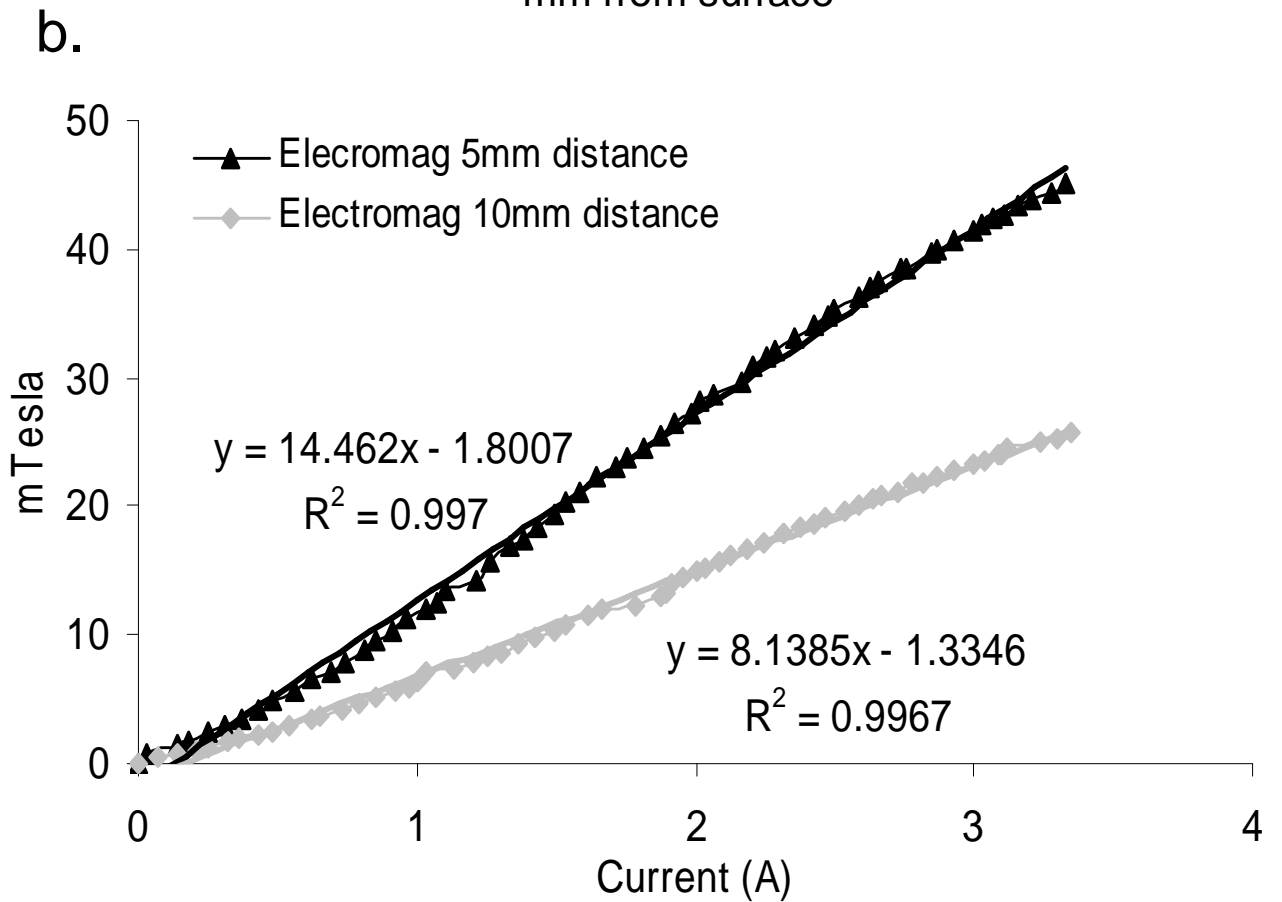
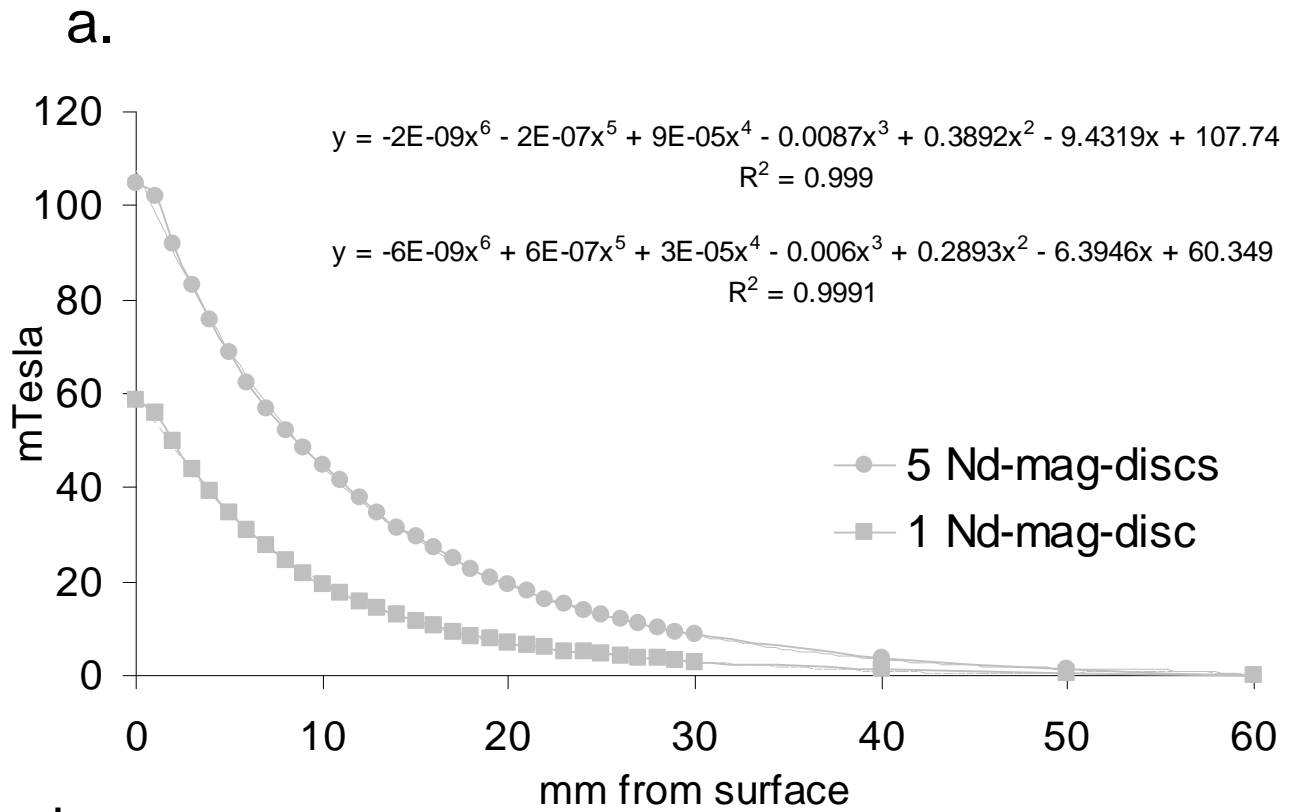
469

470 Fig. 1. Larson et al



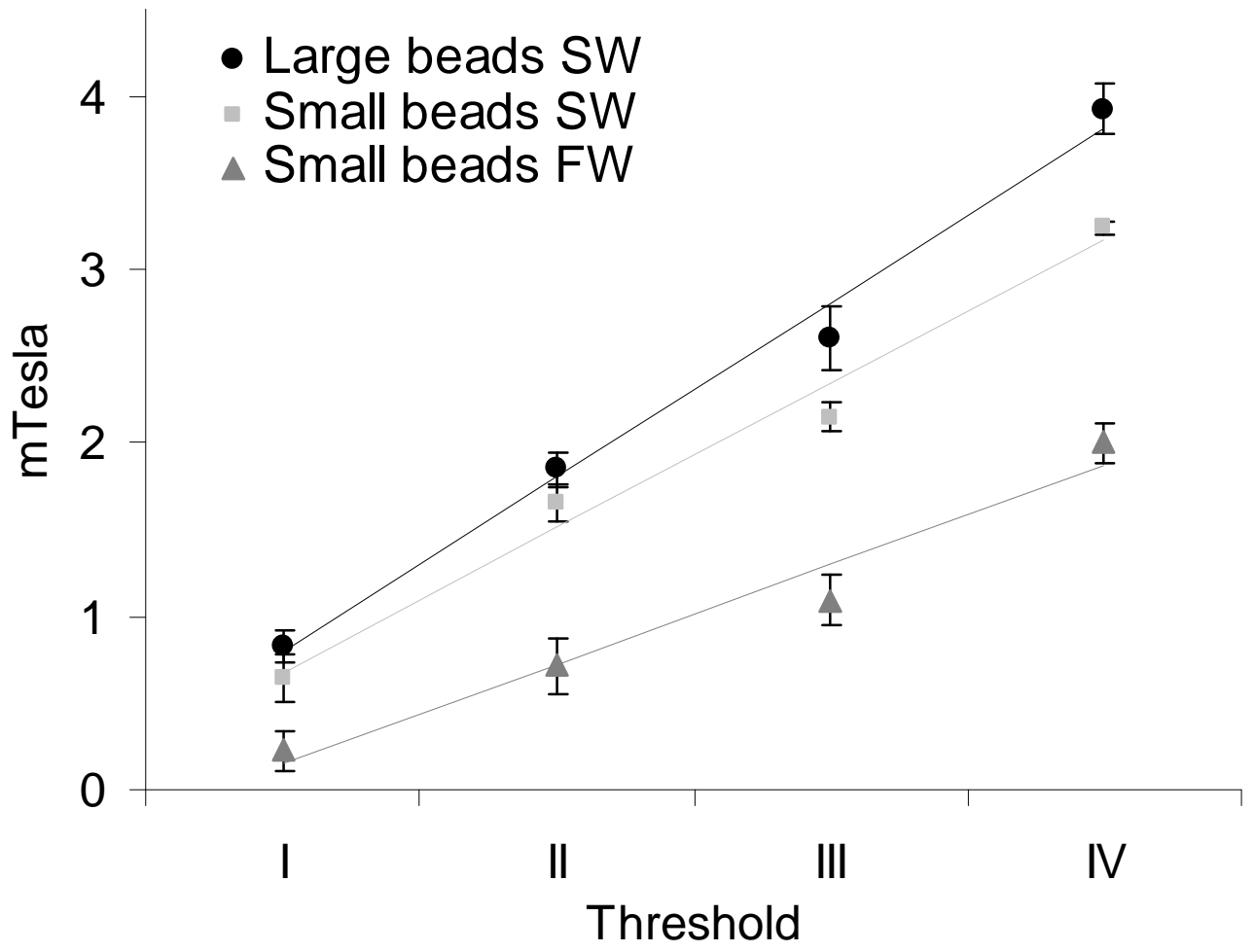
471

472 Fig. 2. Larson et al

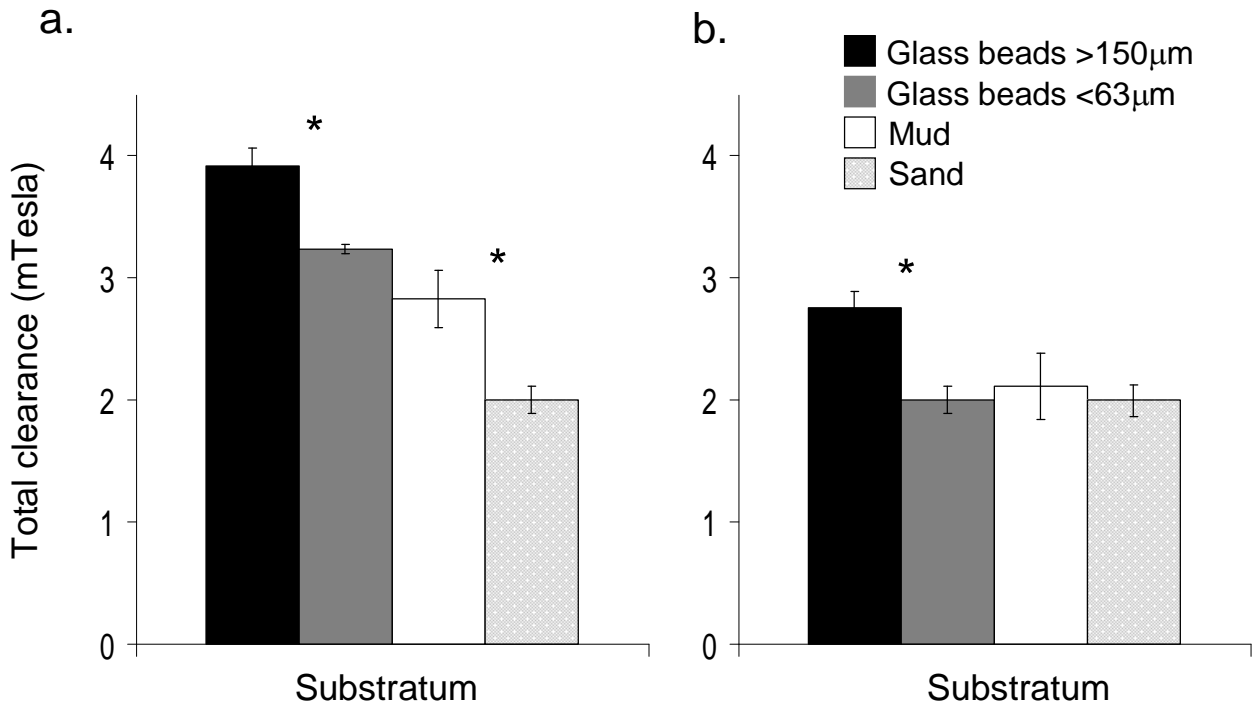


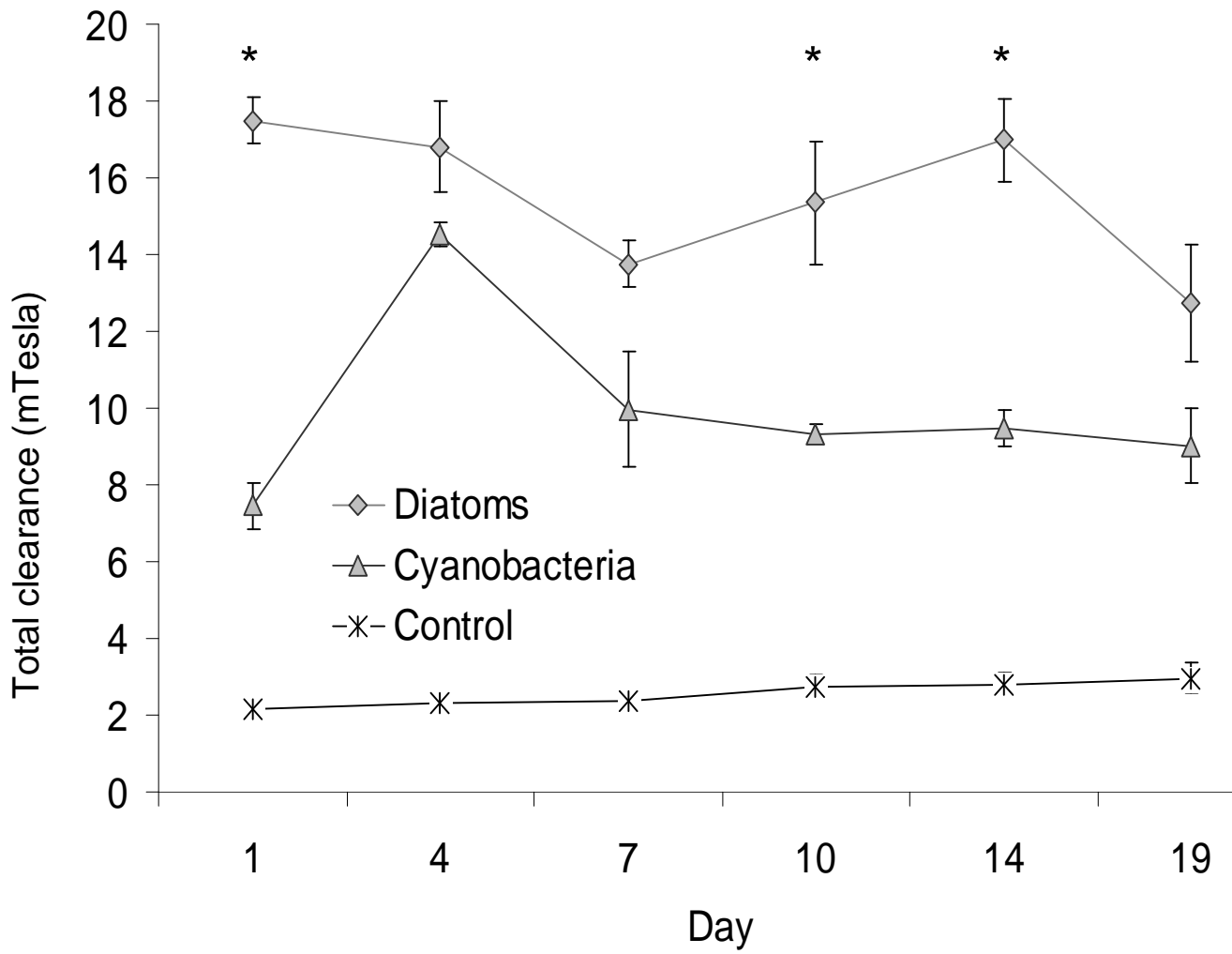
473

474 Fig. 3. Larson et al



477 Fig. 4. Larson et al





510

511 Fig. 6. Larson et al